

Suppression of Spin-Orbit Scattering in Strongly Disordered Gold Nanojunctions

A. Anaya, M. Bowman, and D. Davidović

Georgia Institute of Technology, Atlanta, Georgia 30332, USA

(Received 4 February 2004; published 8 December 2004)

We discovered that spin-orbit scattering in strongly disordered gold nanojunctions is strongly suppressed relative to that in weakly disordered gold thin films. This property is unusual because in weakly disordered films spin-orbit scattering increases with disorder. Granularity and freezing of spin-orbit scattering inside the grains explains the suppression of spin-orbit scattering. We propose a generalized Elliot-Yafet relation that applies to a strongly disordered granular regime.

DOI: 10.1103/PhysRevLett.93.246604

PACS numbers: 72.25.Rb, 72.25.Ba, 73.21.La, 73.23.-b

The field of spintronics has recently emerged as a potential alternative to conventional charge-based electronics [1]. What sets spintronics apart is the explicit study or use of the electron spin degree of freedom. A challenge in spintronics is the finite lifetime of spin-polarized current, since electron spins can flip in normal metals and semiconductors.

It is generally accepted that a spin-orbit (SO) interaction, through the so-called Elliot-Yafet mechanism [2,3], causes spin-flip scattering in weakly disordered metals. In this mechanism, the SO scattering time (τ_{SO}^{EY}) is proportional to the momentum relaxation time τ , $\tau_{SO}^{EY} = \tau/\alpha$, which is known as the Elliot-Yafet relation. The scattering ratio $\alpha \ll 1$ represents the spin-flip probability during the momentum relaxation time. It depends on the atomic number, band structure, and, to a lesser extent, on sample preparation techniques. It has recently been demonstrated that the Elliot-Yafet relation agrees with measured SO scattering time in a wide range of weakly disordered metallic samples [4].

In this Letter we investigate SO scattering in strongly disordered metals, that is, in metals where conduction electrons undergo transition into Anderson localized states at low temperatures. We find that the relation between disorder and SO scattering time in the strongly disordered regime is qualitatively different from that in the weakly disordered regime. We observe a strong enhancement of the SO scattering time compared to that in weakly disordered samples. We propose that the enhancement of the SO scattering time arises from granularity, as follows.

Consider a 3D granular system composed of grains with average diameter D and average grain-to-grain resistance R_g . If R_g is larger than $R_Q = h/e^2 = 25.8$ k Ω , within a factor of order one, then the system is strongly disordered. If $R_g < R_Q$, within a factor of order one, then the system is weakly disordered [5].

By definition, R_g is larger than the resistance inside the grains. The dwell time of an electron on any given grain (t_D) is roughly $t_D = t_H R_g / R_Q$, where $t_H = h/\delta$ is the Heisenberg time (δ is the level spacing).

We consider strongly disordered granular samples that do not exhibit Coulomb blockade at low temperatures. The electron localization length in these samples is larger than the sample size, and electrons at the Fermi level are spatially extended through the sample. The conditions for the absence of Coulomb blockade at low temperature are discussed in more detail later in the text.

We discuss SO scattering time of electrons at the Fermi level and at zero temperature. We assume that the grains are ballistic so that momentum relaxation is dominated by surface scattering. So the Elliot-Yafet relation predicts a SO scattering time of $\tau_{SO}^{EY} = D/(\alpha v_F)$. We argue that τ_{SO}^{EY} is not a good estimate of the spin-orbit scattering time if the grains are sufficiently small and R_g is large enough.

If the grains were completely isolated, then the strength of SO interaction would be governed by a dimensionless parameter t_H/τ_{SO}^{EY} , and SO scattering inside the grains would be weak if $t_H < \tau_{SO}^{EY}$ [6,7]. In this case, the electronic wave functions of the grain would be nearly all spin-up or all spin-down.

Reducing the grain diameter decreases both t_H and τ_{SO}^{EY} , as $t_H \sim \frac{D^3}{v_F \lambda_F^2}$ and $\tau_{SO}^{EY} \sim \frac{D}{\alpha v_F}$, respectively. Since t_H decreases faster than τ_{SO}^{EY} , a borderline diameter D^* exists, below which SO scattering is weak. From $t_H \sim \tau_{SO}^{EY}$, we obtain $D^* = \lambda_F/\sqrt{\alpha}$.

In a granular system, as in Fig. 1(a), once an electron is localized within any given grain its motion is governed by the wave functions of the grain. If $D < D^*$, the spin-

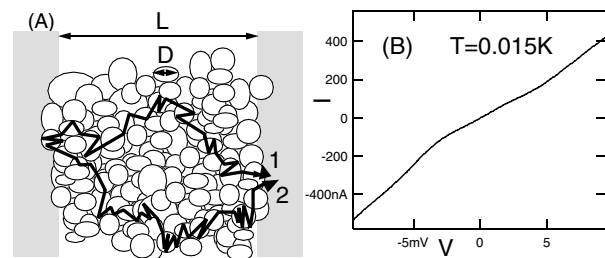


FIG. 1. (a) Sketch of a granular sample and two semiclassical electron trajectories traversing the sample. (b) I - V curve of a sample smaller than the localization length.

flip probability inside the grain would be small, even if $t_D > \tau_{SO}^{EY}$, because SO scattering in individual grains freezes after the Heisenberg time [6,7].

Since SO scattering inside the grains with $D < D^*$ is weak, we propose that electrons at the Fermi level at zero temperature may flip spin only when they hop between neighboring grains, with a spin-flip probability α . This leads to an estimate

$$\tau_{SO} = \frac{t_D}{\alpha} \sim \frac{D^3}{\alpha v_F \lambda_F^2} \frac{R_g}{R_Q}. \quad (1)$$

This equation generalizes the Elliot-Yafet relation for granular systems. An interesting feature of this equation is that the SO scattering time is proportional to the resistance between grains. The resistivity is $\rho \sim R_g D$, hence an increase in resistivity leads to an increase in SO scattering time, a behavior opposite to that found in weakly disordered homogeneous metals, since τ_{SO} is enhanced at the expense of dwell time.

We use electron transport in strongly disordered gold nanojunctions to investigate SO scattering in the strongly disordered regime. An image of one nanojunction, from a scanning electron microscope, is shown in Fig. 2(a). We create these nanojunctions by making electric contacts between two Au films at large bias voltage [8,9].

To summarize, Au atoms are deposited in high vacuum over two bulk Au films separated by a ~ 70 nm slit, as sketched in Fig. 2(b). The applied voltage is 10 V and the current is measured during the deposition, to detect the moment of contact, at which point the evaporation is stopped and the voltage is reduced. Large voltage introduces strong disorder in the nanojunction, through processes such as electromigration, surface atom diffusion, and intermixing with H_2O and O_2 molecules [8].

Au films to the left and right of the nanojunction are good metals with resistivity $\approx 35 \mu\Omega \text{ cm}$. Using a combination of scanning electron microscopy and *in situ* transport measurements, we determined that the nanojunctions were homogeneous at a length scale comparable to the gap size (we determined that the sample resistance was inversely proportional to width w in Fig. 1). The resistivity of the material inside the nanojunction was estimated to be $\rho \approx 10^5 \mu\Omega \text{ cm}$ [9]. This value is larger than the so called “maximum metallic resistivity” of

$200 \mu\Omega \text{ cm}$. Thus, the nominal transport mean free path (l), obtained from $\rho = mv_F/ne^2l$, is $l \approx 0.01 \text{ \AA}$, much shorter than the Fermi wavelength.

The short mean free path indicates that Au in the nanojunction is very disordered. We have explained the disorder by granularity and the grain size much smaller than the nanojunction dimensions [9]. In particular, the disorder could not be amorphous as Au did not alloy with the impurities that were present in sample fabrication (H_2O or O_2). Our imaging resolution, however, was insufficient to determine the grain diameter. Recently, it has been demonstrated that the large bias voltages applied to Au surfaces induce electrochemical processes that lead to formation of Au nanoparticles of diameter on the order of a few nanometers [10,11], and these nanoparticles were self-assembling into a granular structure [11].

In the prior work [9], we showed that the electron localization length in the nanojunction is finite at low temperatures. To summarize, samples with resistance larger than approximately R_Q displayed Coulomb blockade. The width of these samples was smaller than approximately 50 nm. The Coulomb blockade was attributed to electron tunneling on and off the localized electronic wave functions inside the junction. From the temperature dependence of the conductance in the Coulomb blockade, we determined that the localization length exceeded 20 nm.

In addition, samples with resistance smaller than about $0.5R_Q$ did not exhibit Coulomb blockade at $T = 0.015 \text{ K}$. The I - V curve of these samples at $T = 0.015 \text{ K}$ was Ohmic, i.e., it was linear around zero bias voltage. The dependence of the Coulomb blockade on sample resistance in our nanojunctions was analogous to that found in strongly disordered InO_x mesoscopic semiconductors [12].

The absence of Coulomb blockade in low resistance samples suggested that the localization length exceeded the nanojunction length. In this regime, the electronic wave functions extend from one reservoir to another and quantum electron transport can be described using models based on weak-disorder theories. In this Letter, we select these low resistance samples to investigate SO scattering, because quantum interference effects are easier to interpret in the low resistance samples.

Note that in a granular system the nominal transport mean free path obtained from Drude resistivity can be much shorter than the Fermi wavelength, even in the metallic state at zero temperature [13]. Thus, it is not unphysical that the localization length is larger than the nanojunction length (despite the fact that the nominal mean free path is $\ll \lambda_F$).

The standard technique to measure τ_{SO} in disordered conductors is weak localization [14], the effect that originates from the orbital effect of the applied magnetic field on the electron wave functions. In our samples, however, the nominal transport mean free path is shorter than λ_F ,

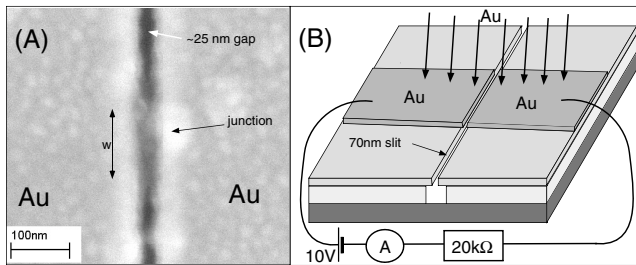


FIG. 2. (a) Image of a strongly disordered Au nanojunction. (b) Fabrication of strongly disordered Au nanojunctions.

and we show that in this case the Zeeman effect is stronger than the orbital effect. We then introduce a new technique to measure a τ_{SO} lower bound.

We find that τ_{SO} lower bound varies weakly among low resistance samples, down to resistance below $0.1R_Q$. The I - V curve of sample 2 [Fig. 1(b)] is linear at zero bias voltage. It has only a weak suppression of differential conductance near zero bias voltage, which is a Coulomb-blockade precursor [8].

A lock-in technique, with a $2 \mu\text{V}$ excitation voltage, measures the differential conductance (G). Figure 3 shows G versus B in samples 1 and 2. The conductance clearly exhibits fluctuations with the magnetic field. The fluctuations are consistent with universal conductance fluctuations or what are known as magnetofingerprints, because (1) the amplitude of the fluctuations is $\sim e^2/h$, (2) fluctuations are reproducible with field sweep, and (3) fluctuations are uncorrelated when samples are thermally cycled.

Magnetofingerprints in our samples differ from those in weakly disordered metals, in that they are caused by the Zeeman effect, not by the Aharonov-Bohm effect. The gray-scale image in Fig. 4 displays differential conductance versus bias voltage and magnetic field [$G(V, B)$]. The main signature of the data is a structure in conductance which shifts linearly with V and B , with pronounced lines in V - B parameter space. Some of the lines are highlighted with dashed lines of the form $eV \pm 2\mu_B B = \text{const}$. By comparison, in weakly disordered metallic samples where the mean free path is longer than the Fermi wavelength, the fluctuations with field and the fluctuations with voltage are uncorrelated. [14]

Consider quantum interference among two semiclassical electron pathways through the sample, depicted in Fig. 1(a). The interference depends on the phase difference ϕ between the probability amplitudes of the trajectories, and can be constructive or destructive, depending on whether $\phi = 2n\pi$ or $\phi = (2n + 1)\pi$, where $n = 0, \pm 1, \dots$. For reference, we recall that the characteristic magnetic field for the Aharonov-Bohm effect is given by

the field for a flux quantum $\Phi_0 = h/2e$ over the sample area, $B_{AB} = \Phi_0/L^2$ [14].

In a magnetic field, Zeeman splitting causes spin-up and spin-down electrons to have different Fermi wavelengths, hence a spin-dependent contribution to ϕ . We find the contribution is $\sigma\mu_B B(t_2 - t_1)/\hbar$, where $\sigma = \pm 1$ corresponds to the spin direction and $t_{1,2}$ are the times of flight along the trajectories. Typical times of flight are $L^2/v_F l$, where l is the transport mean free path. The Zeeman effect becomes significant when $\phi \sim 1$, and the characteristic field for the Zeeman effect is $B_Z = \frac{l}{\lambda_F} \frac{\Phi_0}{L^2}$. Thus, conductance fluctuations are spin based if $B_Z/B_{AB} = l/\lambda_F < 1$. Our sample parameters are such that $B_Z/B_{AB} = l/\lambda_F < 1$.

If the bias voltage is nonzero, then electrons injected from the Fermi level have a voltage-dependent contribution to ϕ , which is $\int_0^{t_1} eV(t)dt/\hbar - \int_0^{t_2} eV(t)dt/\hbar$. In homogenous samples, which is true at a length scale bigger than grain size, the voltage drop is linear in space, and the contribution becomes $eV(t_1 - t_2)/(2\hbar)$. Thus,

$$\phi = eV(t_1 - t_2)/(2\hbar) + \sigma\mu_B B(t_1 - t_2)/\hbar.$$

For any given pair of trajectories, the voltage-dependent contribution is proportional to the spin-dependent contribution. It follows that if both V and B are varied with a constraint that $eV + \sigma 2\mu_B B = \text{const}$, then the interference of an electron with spin σ is unchanged. As a result, the conductance of electrons with spin σ is constant when $eV + \sigma 2\mu_B B = \text{const}$, explaining Fig. 4.

We have neglected SO scattering in the analysis. In the following paragraphs, we take SO scattering into account. SO scattering does not destroy phase coherence [15] and we need to obtain ϕ in the presence of SO scattering.

Assume SO scattering to be strong, $\tau_{SO} \ll t$, where t is the typical time of flight defined above. In this case, phase coherence survives only in the singlet channel, in which an electron traversing one trajectory with spin-up interferes with itself after traversing a second trajectory with spin-down. [15] The phase shift in the singlet channel is

$$\phi_{SO} = eV(t_1 - t_2)/(2\hbar) + \sigma\mu_B B(t_1 + t_2)/\hbar.$$

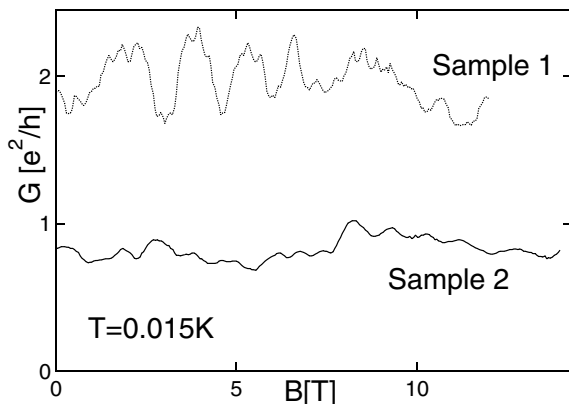


FIG. 3. Differential conductance versus magnetic field.

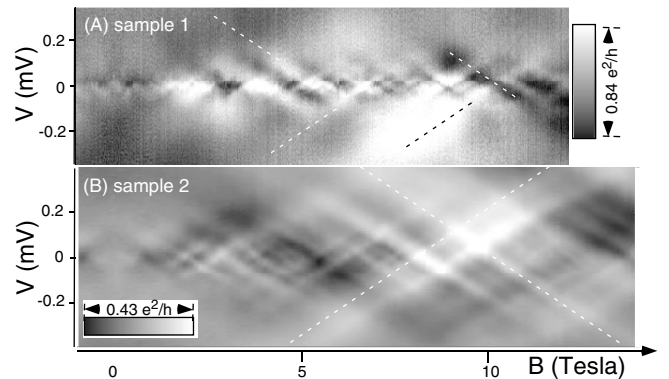


FIG. 4. Differential conductance versus magnetic field and bias voltage in samples 1 and 2 at $T = 0.015$ K.

Hence, the voltage-dependent contribution to the phase is not proportional to the field-dependent contribution. The ratio of these two contributions varies randomly among different pairs of trajectories. So fluctuations in conductance versus field should be uncorrelated with fluctuations in conductance versus voltage. However, Fig. 4 is contrary to what one would expect for strong SO scattering ($\tau_{\text{SO}} \ll t$). It follows then that the SO scattering is not strong ($\tau_{\text{SO}} > t$).

The typical time of flight (t) can be obtained from the correlation energy (E_C), as $E_C = h/t$. E_C is the interval of electronic energies within which the electronic wave functions are correlated in space and equally contribute to conductance fluctuations. It can be measured from the correlation voltage (V_C) as $E_C = V_C/e$ [14], which is the characteristic voltage scale for the fluctuations in conductance with bias voltage. V_C is roughly equal to the spacing between lines in Fig. 4 along the direction parallel to the bias-voltage axes.

The correlation voltage is obtained numerically from the voltage correlation function $Y(V)$, as $Y(V_C) = 0.5Y(0)$, where $Y(V) = \overline{G(V, B')G(0, B') - G(V, B')G(0, B')}$ and averaging is over B' . We obtain $V_C(0) = 31$ and $104 \mu\text{V}$ in samples 1 and 2, respectively. It follows that $\tau_{\text{SO}} > 1.3 \times 10^{-10}$ s and $\tau_{\text{SO}} > 4 \times 10^{-11}$ s in samples 1 and 2, respectively. By comparison, τ_{SO} measured in weakly disordered gold films with resistivity $\rho \approx 66 \mu\Omega \text{ cm}$ is 1.9×10^{-13} s [16], at least 3 orders of magnitude shorter than τ_{SO} in our nanojunctions. This is the main finding of this Letter.

The suppression of SO scattering in our samples can be explained by the granular model described in the introduction. We extract α from τ_{SO} measured by weak localization in thin films of Au, [16] $\alpha \approx 5 \times 10^{-3}$. In this case we obtain $D^* \sim \lambda_F/\sqrt{\alpha} \approx 7$ nm. The scattering ratio α can also be extracted from energy level spectroscopy of nanometer scale Au grains [17]. In this case, we find that α varies among different grains, $0.01 < \alpha < 0.05$. Thus $2.2 \text{ nm} < \lambda_F/\sqrt{\alpha} < 5$ nm. For example, assume $D = 4$ nm and $\alpha = 0.01$. From resistivity we obtain $R_g \approx \rho/D = 2.5 \times 10^5 \Omega$, and Eq. (1) predicts $\tau_{\text{SO}} \approx 3.4 \times 10^{-10}$ s.

In conclusion, we have demonstrated that the magneto-fingerprints in strongly disordered Au nanojunctions are spin based. The signature of spin-based magnetofingerprints is a structure in conductance that shifts linearly with bias voltage and magnetic field. The linear structure requires that the transport time (or the dephasing time) be shorter than or comparable to the SO scattering time, which we use to estimate a lower bound of the SO scattering time. The SO scattering time in strongly disordered samples is enhanced by at least 3 orders of magnitude relative to that in weakly disordered thin films. Granularity suppresses spin-orbit scattering when the grains are weakly coupled. We propose a generalization

of the Elliot-Yafet relation that applies to strongly disordered granular samples and that agrees with our observations.

As a final note, electron spins confined in quantum dots have been proposed as candidate quantum bits, because spin is stable for zero-dimensional systems [18]. In this Letter, we show that, without quantum dots, a distributed strongly disordered system has a similar spin stability. This may be an alternate route for the fabrication of solid-state devices with high spin stability.

We thank A. L. Korotkov for useful discussions. This work was performed in part at the Cornell Nanofabrication Facility (a member of the National Nanofabrication Users Network), which is supported by the NSF under grant no. ECS-9731293, Cornell University and Industrial affiliates, and the Georgia-Tech electron microscopy facility. This research is supported by the David and Lucile Packard Foundation grant no. 2000-13874 and the NSF grant no. DMR-0102960.

-
- [1] S. A. Wolf, D. D. Awschalom, R. A. Buhrman, J. M. Daughton, S. von Molnar, M. L. Roukes, A. Y. Chtchelkanova, and D. M. Treger, *Science* **294**, 1488 (2001).
 - [2] R. J. Elliot, *Phys. Rev.* **96**, 266 (1954).
 - [3] Y. Yafet, *Solid State Phys.* **14**, 1 (1963).
 - [4] F. J. Jedema, M. S. Nijboer, A. T. Filip, and B. J. van Wees, *Phys. Rev. B* **67**, 085319 (2003).
 - [5] I. S. Beloborodov, K. B. Efetov, A. V. Lopatin, and V. M. Vinokur, *Phys. Rev. Lett.* **91**, 246801 (2003).
 - [6] P. W. Brouwer, X. Waintal, and B. I. Halperin, *Phys. Rev. Lett.* **85**, 369 (2000).
 - [7] K. A. Matveev, L. I. Glazman, and A. I. Larkin, *Phys. Rev. Lett.* **85**, 2789 (2000).
 - [8] A. Anaya, A. L. Korotkov, M. Bowman, J. Waddell, and D. Davidović, *J. Appl. Phys.* **93**, 3501 (2003).
 - [9] M. Bowman, A. Anaya, A. L. Korotkov, and D. Davidović, *Phys. Rev. B* **69**, 205406 (2004).
 - [10] F. J. R. Nieto, G. Andreasen, M. E. Martins, F. Castez, R. C. Salvarezza, and A. J. Arvia, *J. Phys. Chem. B* **107**, 11452 (2003).
 - [11] J. E. Grose, B. Ulgut, A. N. Pasupathy, H. D. Abruna, and D. C. Ralph, (to be published).
 - [12] V. Chandrasekhar, Z. Ovadyahu, and R. A. Webb, *Phys. Rev. Lett.* **67**, 2862 (1991).
 - [13] Y. Imry, *Introduction to Mesoscopic Physics* (Oxford University Press, New York, 1997).
 - [14] S. Washburn and R. A. Webb, *Rep. Prog. Phys.* **55**, 1311 (1992).
 - [15] B. L. Altshuler and A. G. Aronov, in *Electron-Electron Interactions in Disordered Systems*, edited by A. L. Efros and M. Pollak ((North-Holland, Amsterdam, 1985).
 - [16] G. Bergman, *Z. Phys. B* **48**, 5 (1982).
 - [17] J. R. Petta and D. C. Ralph, *Phys. Rev. Lett.* **87**, 266801 (2001).
 - [18] A. V. Khaetskii and Y. V. Nazarov, *Phys. Rev. B* **61**, 12639 (2000).